https://doi.org/10.5194/egusphere-2023-2546
Preprint. Discussion started: 10 November 2023

Biases in ice sheet models from missing noise-induced drift

Alexander A. Robel[1,*], Vincent Verjans[1,2,*], and Aminat A. Ambelorun[1]

[1]School of Earth and Atmospheric Sciences, Georgia Institute of Technology, Atlanta, GA, USA
[2]Center for Climate Physics, Institute for Basic Science, Busan, Republic of Korea
[*]Both authors equally contributed to this study

Correspondence: Alexander A. Robel (robel@eas.gatech.edu)

Abstract. Most climatic and glaciological processes exhibit internal variability, which is omitted from many ice sheet model simulations. Prior studies have found that climatic variability can change ice sheet mean state. We show in this study that variability in frontal ablation of marine-terminating glaciers changes the mean state of the Greenland Ice Sheet through noise-induced drift. Idealized simulations and theory show that noise-induced bifurcations and nonlinearities in variable ice sheet processes are likely the cause of the noise-induced drift in marine ice sheet dynamics. The lack of such noise-induced drift in spinup and transient ice sheet simulations is a potentially omnipresent source of bias in ice sheet models.

1 Introduction

The Earth system exhibits internal variability in many processes on a wide range of time scales. As one component of the Earth system, ice sheets are subject to variability in climatic processes, including snowfall, atmospheric temperatures, and ocean currents. Ice sheets also exhibit internal variability of their own, in processes related to hydrology, ice fracture and ice flow. In general, numerical ice sheet modeling studies focus on the ice sheet response to changes in the mean forcing, often without including internal variability in climate or glaciological systems (e.g., Golledge et al., 2015; DeConto et al., 2021). The central assumption of such studies is that the mean state of glaciers and ice sheets are set only by the mean state of climate and glaciological forcing processes. Several recent studies, most using idealized glacier and ice sheet models, have demonstrated that this assumption may not hold in many circumstances known to exist in the real world. In land-based ice sheets with stochastic variability of surface temperature (Mikkelsen et al., 2018; Lauritzen et al., 2023) or marine-based ice sheets with periodic variability in ice viscosity (Hindmarsh and Le Meur, 2001), stochastic variability of ice shelf length (Robel et al., 2018), or seasonal variability of the calving front (Felikson et al., 2022), the inclusion of variability causes drift of the mean ice sheet state. This phenomenon of "noise-induced drift" is well known in the statistical physics community, where many useful mathematical tools have been developed to understand the cause of this phenomenon (e.g., Kloeden and Platen, 1995; Horsthemke and Lefever, 1984). In this study, we show that noise-induced drift is expected in real ice sheets and any numerical modeling of ice sheets. This is demonstrated with ensemble simulations of the Greenland ice sheet, resembling modern conditions with realistic stochastic forcing. We categorize the three different potential mechanisms of noise-induced drift in generic stochastic systems, and identify which of these mechanisms are likely to cause noise-induced drift in real ice

https://doi.org/10.5194/egusphere-2023-2546
Preprint. Discussion started: 10 November 2023

sheets. We close by arguing that all modern ice sheet models omitting variability in climate and glaciological processes produce biased estimates of the ice sheet mean state and the ice sheet response to climate change.

2 The Greenland Ice Sheet Under Variable Forcing

The central goal of this study is to demonstrate that the mean state of ice sheets depends on the inclusion and magnitude of variability in climate and glaciological processes. To achieve this goal, we run four ensembles of Greenland ice sheet simulations using the Stochastic Ice Sheet and Sea Level System Model (StISSM; Verjans et al., 2022). The core of this model is ISSM, which solves for the ice thickness and velocity on a finite-element mesh refined in locations of interest (Larour et al., 2012). In this study, we use the Shallow Shelf Approximation (SSA; MacAyeal, 1989) and refine the mesh at 11 marine-terminating glacier catchments where the ice sheet margin evolves dynamically. All simulations are initialized at a deterministic steady-state. This configuration is meant to resemble the modern state of the Greenland ice sheet, but deviates somewhat from the real ice sheet which is not at a steady-state (Otosaka et al., 2022). This initial deterministic steady-state comes from a long spin-up run over 31,000 years with temporally constant forcing in surface mass balance (SMB), ablation at calving fronts, and subglacial water pressure (described in more detail in Verjans et al., 2022). SMB at model mesh elements is set according to an elevation-dependent profile which is fit in each glacier catchment to resemble mean 1961-1990 SMB simulated in RACMO2 (Ultee et al., 2023; Ettema et al., 2009). Each marine-terminating catchment has a prescribed rate of ocean melt at calving fronts, based on thermal forcing from Wood et al. (2021). In the spinup, calving rates at each catchment are calibrated to produce a steady-state ice sheet configuration resembling the present-day ice sheet. We apply the Budd sliding law (Budd et al., 1979):

$$\boldsymbol{\tau_b} = -C^2 \boldsymbol{u_b} N, \tag{1}$$

where $\boldsymbol{\tau_b}$ is the basal friction, $\boldsymbol{u_b}$ is the basal sliding speed, C^2 is a space-varying coefficient , and N is the effective pressure. Effective pressure is set to maintain local hydrostatic equilibrium with the ocean throughout the ice-covered model domain (Tsai et al., 2015). The model domain is split into 19 glacier catchments, as defined by Zwally et al. (2012). Initialized from this steady-state, a deterministic control run with temporally constant forcings, exhibits an increase in ice mass by only 0.07% in 2000 years.

We run ensembles of ten member simulations each, applying stochastic variability separately in SMB, calving rate, and subglacial water pressure, and we quantify the role of each forcing in setting the ice sheet mean state. Realistic stochastic parameterizations for SMB and ocean thermal forcing (which determines frontal melt) have been described in previous studies (Ultee et al., 2023; Verjans et al., 2023). In this study, for ease of interpretability, we apply simple white noise to different forcing variables with mean that remains constant in time and equal to deterministic steady-state values. White noise is characterized by independent random perturbations drawn from a Gaussian distribution, and with no autocorrelation in time. For the stochastic SMB and calving ensembles, the standard deviation of the stochastic variable in each catchment is set to 1/3 of the mean in that catchment. This amplitude of variability is chosen for simplicity but is similar to observed variability (Fettweis

https://doi.org/10.5194/egusphere-2023-2546
Preprint. Discussion started: 10 November 2023

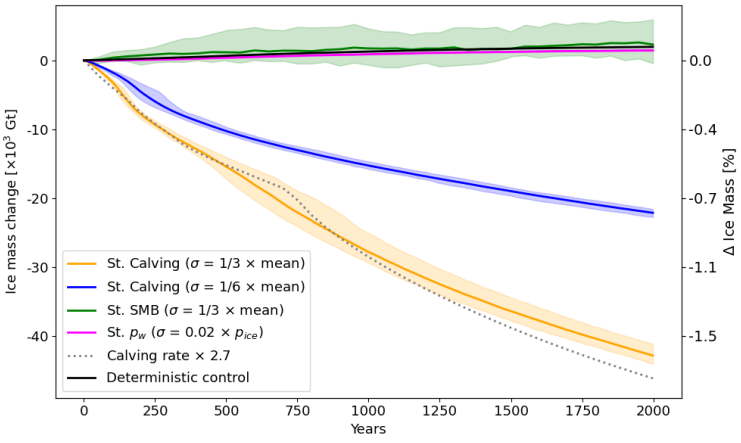

Figure 1. Ensemble mean and range of ice sheet mass change over four stochastic ensembles simulating the Greenland Ice Sheet. Yellow line and shading: white noise variability in calving rate with standard deviation 1/3 of mean. Blue line and shading: white noise variability in calving rate with standard deviation 1/6 of mean. Green line and shading: white noise variability in SMB with standard deviation 1/3 of mean. Magenta line and shading: white noise variability in subglacial water pressure with standard deviation 2% of mean ice pressure at the catchment front. Shadings show the entire 10-member range. Black line is deterministic (i.e. no variability in forcing) simulation. Black dashed line is deterministic but with calving rates multiplied by 2.7.

et al., 2020; Wood et al., 2021). For the stochastic subglacial water pressure ensemble, the standard deviation in catchment-level water pressure is set to just 2% of the mean ice overburden pressure in a region near the glacier front of each catchment, as greater levels of noise lead to numerical instability in the ice sheet model. As a point of comparison, we also run a fourth ensemble with the standard deviation of the stochastic calving rate equal to 1/6 the mean calving rate. Ensemble simulations are run for 2000 years in order to observe the immediate ice sheet response. However, we note that an ice sheet the size of Greenland likely requires more than 10,000 years to reach a new steady-state in response to an ice-sheet-wide change in forcing due to long-term dynamic adjustment extending through the interior. Such long simulations are computationally challenging to perform for the entire Greenland Ice Sheet on a well resolved mesh. The design of this ensemble was initially inspired by the larger Greenland ice sheet ensemble used to benchmark StISSM in Verjans et al. (2022), which showed that just 10 ensemble members are sufficient to constrain the ensemble mean ice sheet mass to less than 0.1% of the converged values (albeit under different stochastic forcing). We also note here that in this depth-averaged model, the dynamic influence of calving and ocean melt at glacier termini is identical. We have chosen to implement stochastic calving in this study, but the results would be identical if stochastic frontal melt were implemented instead.

Figure 1 shows the evolution of Greenland ice sheet mass over time from these ensemble simulations (colored lines and shading) in comparison to the deterministic control simulation (black line). The most striking result is that stochastic variability in calving at marine-terminating glaciers causes substantial drift in the ensemble-mean ice sheet mass (yellow and blue lines). This drift is apparent in all ensemble members and exceeds the spread of intra-ensemble variability after the first few years

https://doi.org/10.5194/egusphere-2023-2546
Preprint. Discussion started: 10 November 2023

of the simulation (i.e., all ensemble members drift almost immediately). At the end of the 2000-year simulation with highest variability amplitude (yellow line), the drift is larger than 1.5% of total initial ice mass. The rate of drift is also approximately proportional to the amplitude of the variability in calving rate. As a point of comparison, the dashed line shows a single simulation, without stochastic variability, but with a 270% increase in the mean calving rate at all 11 marine terminating glaciers for which we simulate terminus migration. This indicates that model drift due to a realistic level of noise in just the annual calving rate is equivalent to ice loss from a substantial increase in calving rate without noise. A deterministic model calibrated to match the observed ice sheet state, which is subject to variability from climatic and glaciological processes, would require tuning far away from true parameter values. We discuss the resulting biases in section 4.

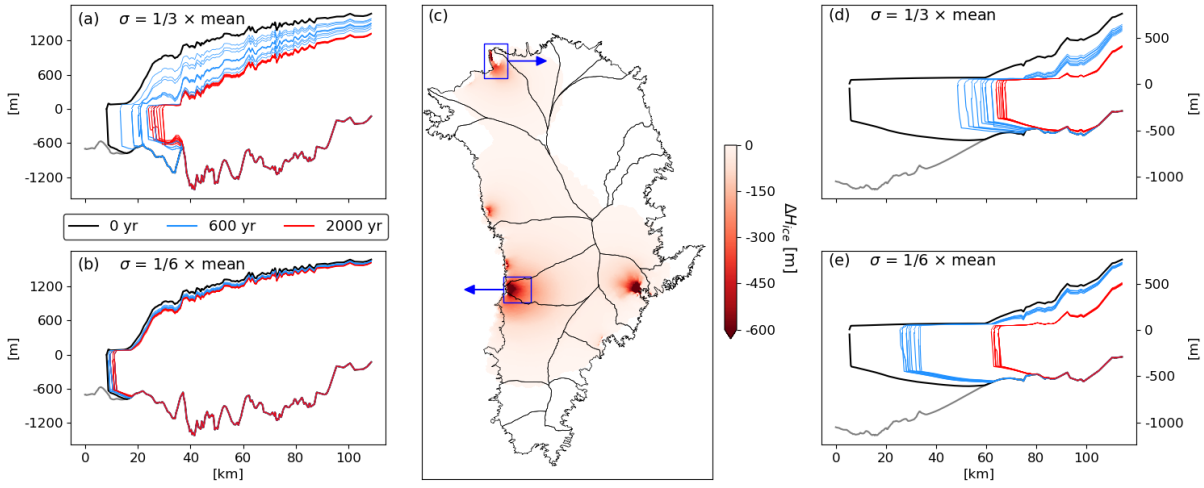

Figure 2. Ice thickness change for stochastic calving ensembles. (a) Profiles of ice thickness for all ensemble members at Sermeq Kujalleq (also called Jakobshavn Isbrae) for high amplitude variability in calving rate. Black line is initial glacier state for all simulations, blue lines are ensemble members after 600 years and red lines are after 2000 years. (b) Same as (a) but for lower amplitude variability in calving rate. (c) Ensemble mean ice thickness change for all of Greenland. (d-e) Same as (a-b) but for Petermann Glacier. Catchment delineations (Zwally et al., 2012) are shown in (c).

In contrast, variability in SMB (green line) does not drive discernible drift in the mean ice sheet volume, in contrast to the study of Lauritzen et al. (2023) which found strong noise-induced drift in an ensemble of Greenland ice sheet simulations in response to temperature variability applied through a positive-degree-day model. We do not use such a model to parameter SMB, instead specifying stochastic variability directly in SMB accumulation/melt rate directly on a catchment-by-catchment basis.

Even with a relatively small level of variability in subglacial water pressure, there is some induced drift (magenta line) in the ice sheet state of all 10 ensemble members. Due to numerical model stability issues, it is not possible to explore whether even higher levels of drift would occur under greater variability in subglacial hydrology with the current experimental design.

https://doi.org/10.5194/egusphere-2023-2546
Preprint. Discussion started: 10 November 2023

While these stochastic ensembles exhibit less than 2% changes in their total Greenland ice sheet mass after 2000 years, the local change in ice thickness at some of the largest marine-terminating glaciers in Greenland is a substantial fraction of their initial ice thickness (Figure 2c). At some glaciers, there is thinning in some ensemble members and thickening at others. At other glaciers, all ensemble members show thinning. To show the expression of this noise-induced drift at different glaciers, we further plot profiles of ice thickness for all ensemble members at Sermeq Kujalleq (also called Jakobshavn Isbrae) in Figure 2a-b and Petermann Glacier in Figure 2d-e. Under a sufficiently large amplitude of variability in calving rate, retreat of the terminus of Sermeq Kujalleq occurs episodically with timing that is variable across ensemble members (Figure 2a). At Petermann Glacier, retreat of the terminus is monotonic and nearly uniform across ensemble members during the early parts of simulations (Figure 2d-e). The different expressions of this drift indicate that there is likely to be more than one mechanism responsible for producing the drift, as explored in the next section.

3 Causes of Noise-Induced Drift in Ice Sheets

Many systems, including the climate system (Penland, 2003), exhibit noise-induced drift, wherein inclusion of noise causes a change in the mean system state. To explain the potential causes of noise induced drift, we start from a generic stochastic differential equation

$$\frac{d\mathbf{x}}{dt} = f(\mathbf{x}) + g(\mathbf{x})\eta(t)^{\beta}, \tag{2}$$

where $\mathbf{x}$ is the model state, t is time, $f(\mathbf{x})$ is a function describing the deterministic model dynamics, $g(\mathbf{x})$ is a function describing how the amplitude of the noise forcing the system may depend on model state, $\eta(t)$ is a random noise term drawn from some distribution (typically Gaussian), and β is an exponent. In the case where $f(\mathbf{x}) = -\alpha\mathbf{x}$, $g(\mathbf{x}) = 1$, $\beta = 1$, and $\eta(t)$ is a random variable drawn from a Gaussian distribution, this is the Langevin equation describing Brownian motion of a particle without drift. However, in many more complex systems, real physical processes described by the components of this equation lead to noise-induced drift. For a more technical review of noise-induced drift, the interested reader is referred to Horsthemke and Lefever (1984).

Here, we describe three causes of noise-induced drift that are potentially relevant to ice sheets:

1. **Noise-induced bifurcation/tipping:** In Equation 2, when $f(\mathbf{x}) = \alpha\mathbf{x}$, α describes the linear stability of the system. If α is negative the system is stable, as perturbations from the noise term $\eta(t)$ will be damped. If α is positive the system is unstable as perturbations from the noise term $\eta(t)$ will not be damped. Thus, if a noise perturbation causes α to change sign (i.e., a bifurcation), the system will undergo a transition to a different state. In higher dimensions, α generalizes to a matrix and its eigenvalues characterize the system stability. Such stability properties have been previously explored in the context of ice sheet dynamics where loss of ice sheet stability through the "marine ice sheet instability" or other bifurcations, may be caused by variability in climate forcing (Mulder et al., 2018; Christian et al., 2022; Sergienko and Haseloff, 2023).

https://doi.org/10.5194/egusphere-2023-2546
Preprint. Discussion started: 10 November 2023

2. **Multiplicative noise:** In Equation 2, when $g(\mathbf{x})$ is any function that is not even about the fixed point ($\frac{\partial f}{\partial x}|_{\mathbf{x}=\mathbf{x}_*} = 0$), i.e., $g(\mathbf{x}_* - \eta) \neq g(\mathbf{x}_* + \eta)$. This describes any system where the amplitude of noise perturbations depends on the system state, causing the entire noise term $g(\mathbf{x})\eta(t)$ to have a non-zero mean. Physically, such multiplicative noise arises in systems where there is noise in a term that depends on system state. This has previously been explored in the context of simple glacier models (Mantelli et al., 2016; Robel et al., 2018; Mikkelsen et al., 2018).

3. **Nonlinear or asymmetric noise:** If $\beta \neq 1$ (excluding the trivial case where $\beta = 0$) or if the underlying noise process has non-zero mean (i.e., the distribution of noise is intrinsically "asymmetric"), then the noise term will cause drift in the mean system state. Because most canonical stochastic models assume that the noise term is linear and sampled from a Gaussian distribution, this potential cause of noise-induced drift has received considerably less attention in the literature (although discussed in detail by Horsthemke and Lefever, 1984). Glacier ice is a viscous non-Newtonian fluid, meaning that glacier flow speed exhibit a strong nonlinear sensitivity to many different types of forcing (Glen, 1955; Millstein et al., 2022). Robel et al. (2018) previously considered this source of noise-induced drift in the context of ice shelf buttressing, but many other processes related to ice flow may exhibit similar nonlinear-noise-induced-drift.

To understand the role of these different potential causes of noise-induced drift in ice sheet dynamics, we consider several highly idealized stochastic ensembles. In each simulation, we use StISSM to simulate ice velocity and thickness evolution of a single marine-terminating glacier in a rectangular channel of uniform width, without floating ice. Model configuration choices such as the stress balance approximation and the basal sliding law are identical to the Greenland ensemble described in the previous section, but with spatially uniform basal friction coefficient (C^2). In all configurations, an initial deterministic steady-state is obtained by holding all forcing variables constant and running until the total ice mass of the glacier changes by less than 0.05% in 200 years. In each idealized stochastic ensemble, calving rate is drawn from a Gaussian distribution (i.e., white noise) with mean equivalent to the initial deterministic calving rate and standard deviation equal to 1/3 of the mean. We perform ensemble simulations of 30 members each, running for 2000 years.

3.1 Noise-induced bifurcation/tipping

Figure 3 shows the results of three idealized stochastic ensembles, all of which have the same background prograde slope of 0.004 in bed topography. In the first stochastic ensemble (Figure 3a-b), the bed topography includes a single sinusoidal bump of 100 m height in bed topography at the initial terminus position. Once the stochastic calving begins, 95% of the ensemble members start retreating past the bump within the first 140 years of the simulation. The second ensemble (Figure 3c-d) is identical to the first, except without a bump in bed topography, and the steady-state calving rate used in the spin-up is adjusted to maintain a similar terminus position. Though the initial glacier state is not identical due to the difference in bed topography, it is sufficiently similar that we do not attribute the subsequent behavior to a different glacier state. Instead of retreating, all ensembles members advance in response to stochastic calving. The different response to stochastic forcing between these two ensembles indicates that the ensemble-mean retreat in the first ensemble is caused by the presence of the bump in bed

https://doi.org/10.5194/egusphere-2023-2546
Preprint. Discussion started: 10 November 2023

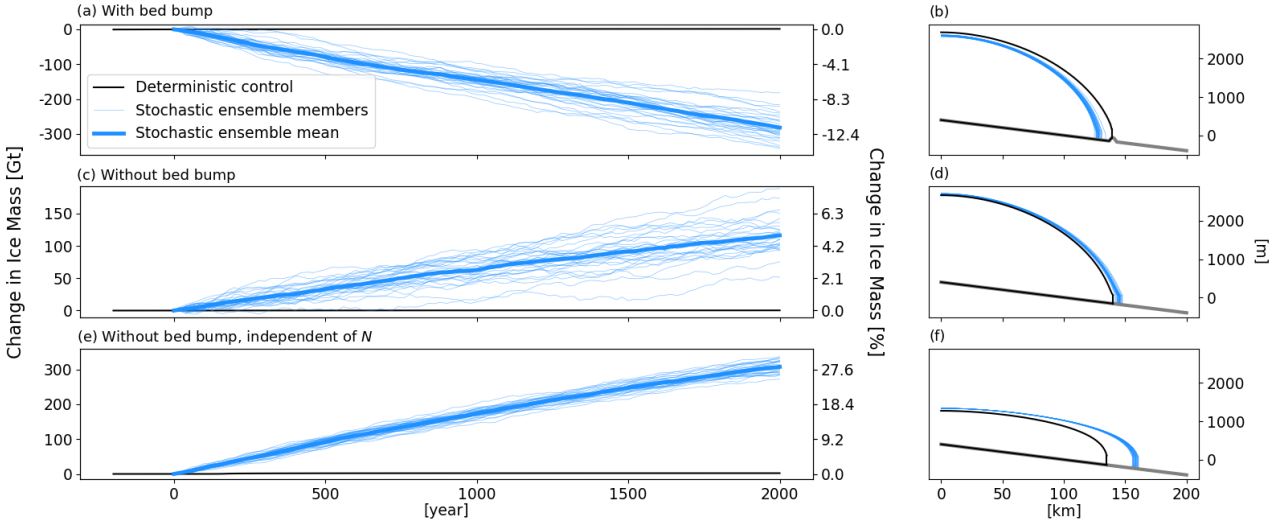

Figure 3. Stochastic ensembles for an idealized marine-terminating glacier in a rectangular channel on a prograde bed slope. (a-b) Including a sinusoidal bed bump. (c-d) Without bed bump. (e-f) Without bed bump and the effective pressure constant in time. Left panels plot change in ice mass over time, right panels show glacier thickness profiles at the end of simulations. In all panels, black line is deterministic control run, thick blue line is stochastic ensemble mean, thin blue lines are all stochastic ensemble members.

topography, which adds a well-understood bifurcation to the system dynamics related to a positive feedback in ice flow with bed depth. This provides a simple example of mechanism #1 identified above: noise-induced bifurcation/tipping.

3.2 Multiplicative noise

Noise-induced tipping is clearly not the only mechanism causing the drift seen in the more realistic simulations discussed in the prior section, since drift still occurs even in the absence of a bifurcation in system dynamics. Multiplicative noise (mechanism #2) may explain this drift in the second stochastic ensemble as variability at the calving front perturbs the near-terminus thickness, causing linear variations in effective pressure and ultimately velocity through the Budd sliding law (Eq. (1)). To investigate this possibility, we consider a stochastic ensemble (Figure 3e-f) in which the effective pressure dependence is removed from Eq. (1), effectively introducing a sliding law linear in sliding velocity only. In this case, drift still occurs, indicating that multiplicative noise through evolving effective pressure is unlikely to be the only mechanism causing the drift. Though ice sheet dynamics involve the complex interplay of many factors, the lack of other obvious multiplicative feedbacks likely to cause a significant asymmetry in the variability of terminus thickness or velocity strongly indicates the drift seen in these two ensembles is mainly caused by a different mechanism: nonlinear noise (mechanism #3 above).

https://doi.org/10.5194/egusphere-2023-2546
Preprint. Discussion started: 10 November 2023

3.3 Nonlinear noise

Though there are many sources of nonlinearity in ice sheet dynamics, the fact that only stochasticity in calving causes drift in the Greenland ensemble of the previous section indicates that it is some nonlinear process specific to the glacier terminus which leads to noise-induced drift in the absence of a bifurcation. Here we give mathematical explanations for the drift in response to stochastic variability in terminus position applying to tidewater glaciers and glaciers with floating ice shelves.

Change in terminus position (L) is determined by

$$\frac{dL}{dt} = u_f - u_c \tag{3}$$

where u_f is ice flow velocity towards the terminus, and u_c is the rate of calving at the terminus. In all stochastic simulations considered in this study, the mean of u_c does not change, and so any changes in the time-averaged terminus position must be the result of changes in mean u_f at the terminus.

For a tidewater glacier, like that simulated in Figure 3, u_f is determined by the momentum balance at the terminus

$$2hA^{-1/n}\left|\frac{\partial u_f}{\partial x}\right|^{1/n-1}\frac{\partial u_f}{\partial x} = \frac{\rho_i g}{2}\left(h^2 - \lambda b^2\right) \tag{4}$$

where h is the terminus thickness, b is the water depth, ρ_i is the ice density, $\lambda = \frac{\rho_w}{\rho_i}$ is the ratio of water to ice density, g is the gravitational acceleration, A is the depth-integrated Glen's flow law rate factor, and n is the Glen's flow law exponent. Perturbations to the mean terminus position may cause perturbations to the glacier thickness and bed depth at the terminus which can be included through a Reynolds decomposition: $h = \langle h\rangle + h'$ and $b = \langle b\rangle + b'$, where all variables enclosed with $\langle\rangle$ are time-averaged and perturbed variables are denoted by $'$. All perturbed variables are drawn from a Gaussian distribution with zero mean. Including these decomposed expressions into the above momentum balance (and simplifying) yields an expression for the strain rate at the terminus in terms of perturbations

$$\frac{\partial u_f}{\partial x} = \frac{A\rho_i^n g^n}{2^{n+1}}\left(\langle h\rangle + h' - \lambda\frac{(\langle b\rangle + b')^2}{\langle h\rangle + h'}\right)^n. \tag{5}$$

The quadratic term in this expression is expanded, and we separate terms with only the mean state in their numerator from those including perturbations in their numerator

$$\frac{\partial u_f}{\partial x} = \frac{A\rho_i^n g^n}{2^{n+1}}\left[\left(\langle h\rangle - \frac{\lambda\langle b\rangle^2}{\langle h\rangle + h'}\right) + \left(h' - \frac{2\lambda\langle b\rangle b'}{\langle h\rangle + h'} - \frac{\lambda b'^2}{\langle h\rangle + h'}\right)\right]^n. \tag{6}$$

We perform a Taylor expansion on the resulting expression in terms of the exponent n keeping in mind that terms involving perturbations will generally be smaller than terms involving on the mean state. Thus, terms depending on higher powers of h' and b' can be ignored, and we only keep the first two terms of the expansion (i.e., linearizing):

$$\frac{\partial u_f}{\partial x} = \frac{A\rho_i^n g^n}{2^{n+1}}\left[\left(\langle h\rangle - \frac{\lambda\langle b\rangle^2}{\langle h\rangle + h'}\right)^n + n\left(\langle h\rangle - \frac{\lambda\langle b\rangle^2}{\langle h\rangle + h'}\right)^{n-1}\left(h' - \frac{2\lambda\langle b\rangle b'}{\langle h\rangle + h'} - \frac{\lambda b'^2}{\langle h\rangle + h'}\right)\right]. \tag{7}$$

We re-arrange this expression to emphasize the relative influences of the mean state and perturbations

$$\frac{\partial u_f}{\partial x} = \frac{A\rho_i^n g^n}{2^{n+1}}\left(\langle h\rangle - \frac{\lambda\langle b\rangle^2}{\langle h\rangle + h'}\right)^n\left[1 + n\left(\langle h\rangle - \frac{\lambda\langle b\rangle^2}{\langle h\rangle + h'}\right)^{-1}\left(h' - \frac{2\lambda\langle b\rangle b'}{\langle h\rangle + h'} - \frac{\lambda b'^2}{\langle h\rangle + h'}\right)\right]. \tag{8}$$

https://doi.org/10.5194/egusphere-2023-2546
Preprint. Discussion started: 10 November 2023

To understand the effect of perturbations on the glacier mean state we take a time average of this expression, which eliminates terms that are linear in a perturbation variable because they have a mean of zero

$$\frac{\partial u_f}{\partial x} = \frac{A\rho_i^n g^n}{2^{n+1}} \left(\langle h \rangle - \frac{\lambda \langle b \rangle^2}{\langle h \rangle} \right)^n \left[1 - \frac{n\lambda \langle b'^2 \rangle}{\langle h \rangle^2 - \lambda \langle b \rangle^2} \right]. \tag{9}$$

If the perturbation terms are drawn from a Gaussian distribution with variance σ^2, then terms involving the square of the perturbation are drawn from a gamma distribution $\Gamma\left(\frac{1}{2}, 2\sigma^2\right)$, which has a non-zero mean equal to σ^2. Thus, the rate of drift depends on how large $n\lambda\sigma_b^2$ is relative to $\langle h \rangle^2 - \lambda \langle b \rangle^2$, where σ_b^2 is the variance of the perturbations in bed depth due to perturbations in ice front position. The sign of this leading order term causing the drift is negative which causes a decrease in the near-terminus strain rate, lower time-averaged u_f and an advance of the terminus, as seen in the simulations in Figure 3c-f. While we might expect that $\sigma_b << \langle b \rangle$, if the bed topography (b_x) is steep, then $\sigma_b = b_x \sigma_L$ (where σ_L is the standard deviation of variability in terminus position) could be a non-negligible fraction of $\langle b \rangle$, causing appreciable drift. Also, if the terminus is at or near flotation, then $\langle h \rangle^2 - \lambda \langle b \rangle^2 \approx \lambda^2 \langle b \rangle^2 - \lambda \langle b \rangle^2 \approx 0.1 \langle b \rangle^2$ and the denominator of the above expression would be sufficiently small to admit significant drift. Given that both steep bed topography and near-flotation termini are common in Greenland, we may expect this effect to be common.

For a glacier with a floating ice shelf, the calving front is not grounded and so the momentum balance does not depend on the bed depth, making the above analysis not applicable. Rather, we consider the effect of buttressing from the floating ice shelf on the velocity of ice through the grounding line. Haseloff and Sergienko (2018) perform an asymptotic analysis to derive an approximation for the ice flow velocity (u_g) though a strongly buttressed grounding line

$$u_g = \left[\frac{(1-\lambda^{-1})\rho_i g}{(1+n^{-1})\Lambda L_s} \right]^n h_g^n \tag{10}$$

where Λ is a parameter governing lateral shear stress within the ice and L_s is the ice shelf length. This expression assumes that ice loss occurs entirely through ablation at the calving front and lateral shear stresses increase linearly across the ice shelf. We consider stochastic calving at the calving front of the floating ice causing Gaussian, zero-mean perturbations to the ice shelf length: $L_s = \langle L_s \rangle + L_s'$. We insert this Reynolds decomposition in the above expression for grounding line flux, and take the Taylor expansion of the resulting expression

$$u_g = \left[\frac{(1-\lambda^{-1})\rho_i g}{(1+n^{-1})\Lambda} \right]^n h_g^n \left(\langle L_s \rangle^{-n} - n\langle L_s \rangle^{-n-1} L_s' + \frac{n(n+1)}{2} \langle L_s \rangle^{-n-2} L_s'^2 + \ldots \right). \tag{11}$$

From this expression, we ignore higher-order terms and rearrange to resemble the original flux expression

$$u_g = \left[\frac{(1-\lambda^{-1})\rho_i g}{(1+n^{-1})\Lambda \langle L_s \rangle} \right]^n h_g^n \left(1 - n\langle L_s \rangle^{-1} L_s' + \frac{n(n+1)}{2} \frac{L_s'^2}{\langle L_s \rangle^2} \right). \tag{12}$$

Taking the time-average, the term which is linear in L_s' vanishes, leaving

$$u_g = \left[\frac{(1-\lambda^{-1})\rho_i g}{(1+n^{-1})\Lambda \langle L_s \rangle} \right]^n h_g^n \left(1 + \frac{n(n+1)}{2} \frac{\langle L_s'^2 \rangle}{\langle L_s \rangle^2} \right). \tag{13}$$

The $L_s'^2$ term is drawn from the $\Gamma\left(\frac{1}{2}, 2\sigma_{L_s}^2\right)$ distribution, which has a non-zero mean equal to $\sigma_{L_s}^2$. Thus, when $\frac{n(n+1)\sigma_{L_s}^2}{2}$ is non-negligible compared to $\langle L_s \rangle^2$, the time-averaged ice flow velocity through the grounding line is increased by stochastic

https://doi.org/10.5194/egusphere-2023-2546
Preprint. Discussion started: 10 November 2023

calving, which will cause the grounding line to retreat. We can note here that different assumptions can be made about the form of lateral shear stress variation across the floating ice shelf or the dominant source of mass loss, and in general the rate of ice flow through the grounding line will be nonlinear in terms of the ice shelf length (Haseloff and Sergienko, 2018), causing the sort of nonlinear-noise induced drift discussed here.

3.4 Attributing causes of drift

Returning to the more realistic Greenland ice sheet ensemble simulations (Figure 2a-b,d-e), we conclude that in most glaciers for which strong noise-induced drift is simulated, there are easily identifiable bed topography features indicating that noise-induced bifurcations are the most common cause of noise-induced drift (as previously argued in Christian et al., 2022). Conversely, there are no tidewater glaciers in this realistic ensemble exhibiting ensemble-average terminus advance due to nonlinearity in hydrostatic stress terms. This is likely because glaciers tend to stabilize at peaks in bed topography (Robel et al., 2022), making it more likely that the sudden onset of stochastic calving would lead to a retreat from noise-induced bifurcation, rather than sustained advance due to the nonlinear-noise mechanism. In contrast, during the earliest stage of Petermann Glacier's retreat (Figure 2e), the bed is entirely prograde and yet ensemble-mean retreat still occurs. Petermann Glacier is one of only two glaciers in Greenland with a buttressing ice shelf remaining. Thus, the mechanism of drift due to nonlinearities in buttressing is likely responsible for the early stages of strong retreat of the Petermann grounding line, before reaching a bed peak, after which a noise-induced bifurcation over a bed peak is likely also playing an important role in the simulated ensemble-mean retreat.

We also note briefly that Lauritzen et al. (2023) find that variability in surface temperature can cause noise-induced drift through a positive-degree-day (PDD) model for SMB, though they do not speculate on the cause of this drift (or refer to it as such). It is likely that the strong nonlinearities in their PDD model are the cause of the noise-induced drift they find in their results, as their simulations do not appear to include bifurcations in SMB or sources of multiplicative noise. Regardless of the precise mechanism of noise-induced drift in different model configurations, our simulations show that there are a range of different mechanisms intrinsic to ice sheet dynamics that cause noise-induced drift to be an expected and essential aspect of realistic simulations of ice sheet evolution.

4 Implications for Ice Sheet Modeling

The noise-induced retreat tendency of the Greenland ensembles simulated in this study indicates that spin-up of an ice sheet model under constant forcing is likely to lead to a modeled ice sheet that is biased compared to observations of real ice sheets, which are naturally subject to noise-induced drift. Such a mismatch is often reduced by tuning, or optimizing model parameter values, including those related to ice sliding, viscosity, calving and ocean melt, through inversion. However, calibrating a parameter to minimize model-observation mismatch arising due to processes not represented in the model may introduce compensating errors in the modeled state. Ice sheet models that tune one parameter to reduce biases in other parameters have been shown to have substantially biased sensitivity to changes in forcing (Berends et al., 2023).

https://doi.org/10.5194/egusphere-2023-2546
Preprint. Discussion started: 10 November 2023

Many contemporary projections of future ice sheet evolution omit variability in forcing for transient projections due to challenges related to modeling ocean circulation near ice sheets or the lack of output from climate models far into the future (Golledge et al., 2015; DeConto et al., 2021). Such an omission may lead the modeled ice sheet sensitivity to future changes to be biased, as noise-induced retreat is an important and realistic component of the forced response. As discussed in the prior section and prior studies (Christian et al., 2022), in the absence of variability, many glaciers may not cross important thresholds to rapid retreat and thus their projected response to climate forcing would be considerably less than is likely in reality. Additionally, potential future changes in the amplitude of variability (e.g., Bintanja et al., 2020) could increase the likelihood of crossing noise-induced bifurcations, and amplify the impacts of state-dependent and asymmetric noise. Such effects cannot be captured if variability in forcing is omitted.

Other contemporary projections of future ice sheet evolution (e.g., the recent ISMIP6 intercomparisons; Goelzer et al., 2020; Seroussi et al., 2020) start from a calibrated initial state, and then simulate the free-running ice sheet state in response to forcing including variability. In such a simulation design, the sudden onset of variability would introduce a transient noise-induced drift. If the sign of the drift is the same as in the ensembles described in section 2, this would cause the projected ice sheet sensitivity to forcing to be too high. Other recent modeling studies use this same spin-up procedure, but then calibrate the ice sheet sensitivity to a changing mean climate with historical observations of ice sheet change (e.g., Nias et al., 2019; DeConto et al., 2021). In such a case, the calibrated sensitivity to changes in the mean climate would be too low, due to the spurious influence of noise-induced drift following the sudden onset of variability in the model. Similarly, the practice of removing "control" simulations with forcing held constant to diagnose ice sheet sensitivity to forcing (Seroussi et al., 2020; Goelzer et al., 2020), may introduce bias due to the lack of noise-induced drift in control simulations.

The potential ice sheet model biases identified here all result from an incomplete representation of variability within climate or glaciological processes. To eliminate or lessen these biases, we recommend including internal variability in the forcing of ice sheet models, both during spin-up and transient simulations. Additionally, improving both glaciological process models (e.g., hydrology and calving) and the efficiency of coupling to climate models, should also yield improvements in the complete and accurate representation of variability. Finally, stochastic ice sheet modeling (e.g., StISSM; Verjans et al., 2022) provides a parallel approach to accurately include variability within ice sheet models in a computationally efficient manner.

Code and data availability. StISSM is an open-source large-scale stochastic ice sheet model that is currently included as part of the public release of ISSM. The public SVN repository for the ISSM code can be found at https://issm.ess.uci.edu/svn/issm/issm/trunk and downloaded using username "anon" and password "anon". The documentation of the code version used here is available at https://issm.jpl.nasa.gov/documentation/ (last access: 30 October 2023). Scripts for the Greenland spin-up simulation follow Verjans et al. (2022) and are available at: https://doi.org/10.5281/zenodo.7144993

https://doi.org/10.5194/egusphere-2023-2546
Preprint. Discussion started: 10 November 2023

Author contributions. AAR conceived the study, developed the theory, and led writing of the manuscript. VV performed the model simulations, post-processed the model output, and contributed to writing. AAA contributed to the mathematical analysis and writing.

Competing interests. The contact author has declared that none of the authors has any competing interests.

290 *Acknowledgements.* This study and all authors are a part of the Stochastic Ice Sheet Project, funded by the Heising-Simons Foundation. Thanks to John Erich Christian and Judith Berner for fruitful discussions during the conception of this study.

https://doi.org/10.5194/egusphere-2023-2546
Preprint. Discussion started: 10 November 2023

References

Berends, C. J., Van De Wal, R. S., Van Den Akker, T., and Lipscomb, W. H.: Compensating errors in inversions for subglacial bed roughness: same steady state, different dynamic response, The Cryosphere, 17, 1585–1600, 2023.

Bintanja, R., van der Wiel, K., Van der Linden, E., Reusen, J., Bogerd, L., Krikken, F., and Selten, F.: Strong future increases in Arctic precipitation variability linked to poleward moisture transport, Science advances, 6, eaax6869, 2020.

Budd, W., Keage, P., and Blundy, N.: Empirical studies of ice sliding, Journal of glaciology, 23, 157–170, 1979.

Christian, J. E., Robel, A. A., and Catania, G.: A probabilistic framework for quantifying the role of anthropogenic climate change in marine-terminating glacier retreats, The Cryosphere, 16, 2725–2743, 2022.

DeConto, R. M., Pollard, D., Alley, R. B., Velicogna, I., Gasson, E., Gomez, N., Sadai, S., Condron, A., Gilford, D. M., Ashe, E. L., et al.: The Paris Climate Agreement and future sea-level rise from Antarctica, Nature, 593, 83–89, 2021.

Ettema, J., van den Broeke, M. R., van Meijgaard, E., van de Berg, W. J., Bamber, J. L., Box, J. E., and Bales, R. C.: Higher surface mass balance of the Greenland ice sheet revealed by high-resolution climate modeling, Geophysical Research Letters, 36, 2009.

Felikson, D., Nowicki, S., Nias, I., Morlighem, M., and Seroussi, H.: Seasonal Tidewater Glacier Terminus Oscillations Bias Multi-Decadal Projections of Ice Mass Change, Journal of Geophysical Research: Earth Surface, 127, e2021JF006 249, 2022.

Fettweis, X., Hofer, S., Krebs-Kanzow, U., Amory, C., Aoki, T., Berends, C. J., Born, A., Box, J. E., Delhasse, A., Fujita, K., et al.: GrSMB-MIP: intercomparison of the modelled 1980–2012 surface mass balance over the Greenland Ice Sheet, The Cryosphere, 14, 3935–3958, 2020.

Glen, J. W.: The creep of polycrystalline ice, Proceedings of the Royal Society of London. Series A. Mathematical and Physical Sciences, 228, 519–538, 1955.

Goelzer, H., Nowicki, S., Payne, A., Larour, E., Seroussi, H., Lipscomb, W. H., Gregory, J., Abe-Ouchi, A., Shepherd, A., Simon, E., et al.: The future sea-level contribution of the Greenland ice sheet: a multi-model ensemble study of ISMIP6, The Cryosphere, 14, 3071–3096, 2020.

Golledge, N. R., Kowalewski, D. E., Naish, T. R., Levy, R. H., Fogwill, C. J., and Gasson, E. G.: The multi-millennial Antarctic commitment to future sea-level rise, Nature, 526, 421–425, 2015.

Haseloff, M. and Sergienko, O. V.: The effect of buttressing on grounding line dynamics, Journal of Glaciology, 64, 417–431, 2018.

Hindmarsh, R. C. and Le Meur, E.: Dynamical processes involved in the retreat of marine ice sheets, Journal of Glaciology, 47, 271–282, 2001.

Horsthemke, W. and Lefever, R.: Noise-induced transitions in physics, chemistry, and biology, Springer, 1984.

Kloeden, P. E. and Platen, E.: Numerical Solutions of Stochastic Differential Equations, https://api.semanticscholar.org/CorpusID:117388744, 1995.

Larour, E., Seroussi, H., Morlighem, M., and Rignot, E.: Continental scale, high order, high spatial resolution, ice sheet modeling using the Ice Sheet System Model (ISSM), Journal of Geophysical Research: Earth Surface, 117, 2012.

Lauritzen, M., Aðalgeirsdóttir, Guðfinna, R. N., Grinsted, A., Noel, B., and Hvidberg, Christine, S.: The influence of inter-annual temperature variability on the Greenland Ice Sheet volume, Annals of Glaciology, pp. 1–8, 2023.

MacAyeal, D. R.: Large-scale ice flow over a viscous basal sediment: Theory and application to ice stream B, Antarctica, Journal of Geophysical Research: Solid Earth, 94, 4071–4087, 1989.

https://doi.org/10.5194/egusphere-2023-2546
Preprint. Discussion started: 10 November 2023

Mantelli, E., Bertagni, M. B., and Ridolfi, L.: Stochastic ice stream dynamics, Proceedings of the National Academy of Sciences, 113, E4594–E4600, 2016.

Mikkelsen, T. B., Grinsted, A., and Ditlevsen, P.: Influence of temperature fluctuations on equilibrium ice sheet volume, The Cryosphere, 12, 39–47, 2018.

Millstein, J. D., Minchew, B. M., and Pegler, S. S.: Ice viscosity is more sensitive to stress than commonly assumed, Communications Earth & Environment, 3, 57, 2022.

Mulder, T., Baars, S., Wubs, F., and Dijkstra, H.: Stochastic marine ice sheet variability, Journal of Fluid Mechanics, 843, 748–777, 2018.

Nias, I. J., Cornford, S. L., Edwards, T. L., Gourmelen, N., and Payne, A. J.: Assessing uncertainty in the dynamical ice response to ocean warming in the Amundsen Sea Embayment, West Antarctica, Geophysical Research Letters, 46, 11 253–11 260, 2019.

Otosaka, I. N., Shepherd, A., Ivins, E. R., Schlegel, N.-J., Amory, C., van den Broeke, M., Horwath, M., Joughin, I., King, M., Krinner, G., et al.: Mass balance of the Greenland and Antarctic ice sheets from 1992 to 2020, Earth System Science Data Discussions, 2022, 1–33, 2022.

Penland, C.: Noise out of chaos and why it won't go away, Bulletin of the American Meteorological Society, 84, 921–925, https://api.semanticscholar.org/CorpusID:122601998, 2003.

Robel, A. A., Roe, G. H., and Haseloff, M.: Response of marine-terminating glaciers to forcing: time scales, sensitivities, instabilities, and stochastic dynamics, Journal of Geophysical Research: Earth Surface, 123, 2205–2227, 2018.

Robel, A. A., Pegler, S. S., Catania, G., Felikson, D., and Simkins, L. M.: Ambiguous stability of glaciers at bed peaks, Journal of Glaciology, 68, 1177–1184, 2022.

Sergienko, O. and Haseloff, M.: 'Stable'and 'unstable'are not useful descriptions of marine ice sheets in the Earth's climate system, Journal of Glaciology, pp. 1–17, 2023.

Seroussi, H., Nowicki, S., Payne, A. J., Goelzer, H., Lipscomb, W. H., Abe-Ouchi, A., Agosta, C., Albrecht, T., Asay-Davis, X., Barthel, A., et al.: ISMIP6 Antarctica: a multi-model ensemble of the Antarctic ice sheet evolution over the 21st century, The Cryosphere, 14, 3033–3070, 2020.

Tsai, V. C., Stewart, A. L., and Thompson, A. F.: Marine ice-sheet profiles and stability under Coulomb basal conditions, Journal of Glaciology, 61, 205–215, 2015.

Ultee, L., Robel, A. A., and Castruccio, S.: A stochastic parameterization of ice sheet surface mass balance for the Stochastic Ice-Sheet and Sea-Level System Model (StISSM v1. 0), EGUsphere, 2023, 1–19, 2023.

Verjans, V., Robel, A. A., Seroussi, H., Ultee, L., and Thompson, A. F.: The stochastic ice-sheet and sea-level system model v1. 0 (STISSM v1. 0), Geoscientific Model Development, 15, 8269–8293, 2022.

Verjans, V., Robel, A., Thompson, A. F., and Seroussi, H.: Bias correction and statistical modeling of variable oceanic forcing of Greenland outlet glaciers, Journal of Advances in Modeling Earth Systems, 15, e2023MS003 610, 2023.

Wood, R. R., Lehner, F., Pendergrass, A. G., and Schlunegger, S.: Changes in precipitation variability across time scales in multiple global climate model large ensembles, Environmental Research Letters, 16, 084 022, 2021.

Zwally, H. J., Giovinetto, M., Beckley, M., and Saba, J.: Antarctic and Greenland Drainage Systems, https://earth.gsfc.nasa.gov/cryo/data/polar-altimetry/antarctic-and-greenland-drainage-systems, 2012.